Phase Separation under a Weak Concentration Gradient

Y. Jayalakshmi,[a] B. Khalil,[b] and D. Beysens

Service de Physique de l'Etat Condensé, Centre d'Etudes de Saclay, F-91191 Gif-sur-Yvette CEDEX, France

(Received 28 May 1992; revised manuscript received 29 September 1992)

Phase separation dynamics is studied in a density-matched liquid mixture in the presence of a weak linear concentration gradient. This novel situation enables nucleation and spinodal decomposition to be studied simultaneously. We observe at all quench depths (i) a central zone of nearly constant concentration width where interconnected domains grow linearly with time, surrounded by (ii) a zone of isolated droplets whose width increases with time, with the droplet growth compatible with a $\frac{1}{3}$ law. These findings suggest generalized nucleation as the phase separation process.

PACS numbers: 64.70.Ja, 05.70.Jk, 64.60.−i

In this Letter we report the phase separation dynamics of a binary liquid mixture under a weak concentration gradient when it is quenched from a temperature at which it is homogeneous to a temperature where it is a two-phase mixture. This is a general process that occurs in many areas of scientific and technological interest such as material science and heat and mass transfer [1–3]. The experiment has been carried out near a critical point where the phase separation behavior can easily be generalized by the use of scaling functions. We have chosen the density-matched mixture cyclohexane (C) + deuterated cyclohexane (C*) + methanol (M) in order to maintain the concentration gradient against gravity-driven convection and to suppress the influence of gravity during phase separation [4]. The phase separation process is expected to proceed [1] through spinodal decomposition (SD) or through nucleation and growth. During SD spontaneous fluctuations grow and generally give rise to interconnected domains. For nucleation and growth an energy barrier exists that prevents the droplets with a radius smaller than a critical radius R^* from growing. Classical theories predict a sharp limiting boundary called the spinodal curve between these two separation processes [2]. However, for real systems, Binder [3] proposes a smooth transition zone (spinodal nucleation) between the two processes at early stages. At late stages, during coarsening, additional effects like hydrodynamic flows in percolating clusters are expected to enhance the growth of the domains for volume fractions exceeding the percolation limit [5]. Wong and Knobler [6] report this expected crossover in the growth exponent from t^1 to $t^{1/3}$ (here t is the time elapsed after the quench) as the volume fraction decreases below 10%.

In the present study the sample is submitted to a weak concentration gradient over its height. This enables the phase separation structures to be observed simultaneously in the unstable and metastable regions for the same quench depth. Our purpose is to determine the concentration dependence of the phase separation structures and the growth laws. In a computer simulation study of spinodal decomposition under concentration gradients, Kolb *et al.* [7] do not see any specific effect of the gradient. Although they do not take into account hydrodynamics in their analysis, we expect a similar insensitivity to the gradient.

The experimental cell is a Helma quartz cell of 2 mm internal thickness, 10 mm width, and 40 mm length and forms a part of the pressure line which is thermally stabilized within ± 1 mK in a water bath. The cell is filled by the sample CC*M at its critical concentration c_c (c_c =0.706 mass fraction of cyclohexane) by displacing mercury. The phase separation is affected by pressure quenches. A differential pressure δP is applied at a temperature held constant at 5 mK above T_c. Our measured value of $dT_c/dP = +34$ mK/bar agrees with the value in the literature [8]. The corresponding quench depth is $\Delta T = (dT_c/dP)\delta P$. At least up to $\delta P = 1$ bar the adiabatic heating is found to be negligibly small. The advantage [9] of the pressure quench over the thermal quench is that the sample reaches the final temperature almost instantaneously, which is an essential criterion for the study of any time-dependent behavior.

Concentration gradients are induced as follows. The homogeneous critical mixture is quenched by ΔT_g below T_c, which at equilibrium leads to a concentration difference Δc_g. After approximately a day the sample shows a flat meniscus. It is then heated to 1 degree above T_c very slowly to reduce convection and mixing and is left for 40 h for diffusion. A smooth concentration gradient develops over the height z of the sample. This system is then cooled over a couple of hours in small temperature steps to 5 mK above T_c. It is then quenched by pressure into the miscibility gap to a temperature $T_c - \Delta T$ where the equilibrium concentration difference is Δc (Fig. 2). An approximate ratio of $\Delta c/\Delta c_g = 0.5$ is maintained to phase separate the sample in the region of linear concentration profile.

The concentration profile over the cell height z is determined just before the pressure quench by a shadow grid technique discussed elsewhere [10]. The concentration difference obtained by integrating the concentration profile over z for a given ΔT_g agrees with that expected from the coexistence curve ($c \times c$) within an experimental resolution of 5%. Absolute concentrations corresponding to

any z are calculated from the parameters of a quadratic fit for the profile around Δc. Here the concentration at the height of the meniscus (z_m) is assumed to be c_c. The sample is imaged by a charge-coupled-device camera. Results of five quenches corresponding to $\Delta T = 2.4$, 4, 12, 25, and 40 mK below T_c are presented here. In all the experiments the concentration gradient $\Delta c_g/\Delta z$ is very weak at the scale of the interface thickness (which is of the order of the correlation length ξ) and at the scale of the domain size L_m, $\Delta c/\xi \gg \Delta c/L_m \gg \Delta c_g/\Delta z$.

A typical phase separation photograph is shown in Fig. 1. At all quench depths we see a central "fast" zone of concentration width Δc_f where phase separation occurs through interconnected structures and is fast. On either side of the fast zone we see two "slow" zones of total width Δc_s where growth and equilibration are slow and the phase separation structures are dropletlike. Beyond the slow zone at the top and bottom of the cell the rest of the liquid remains homogeneous which is expected since $\Delta c_g > \Delta c$. Initially the width Δc_f is almost independent of time; within a short time (dependent on quench depth) a flat meniscus appears at its center. In contrast Δc_s increases with time and saturates at approximately the equilibrium concentration difference Δc. Later, convection rolls appear, indicating the onset of gravity [11].

The slow zone corresponds to nucleation and growth of droplets. The time dependence of its width can be understood by the Langer-Schwartz (LS) nucleation theory [12]. For a quench depth ΔT corresponding to an equilibrium concentration difference Δc, the supersaturation x can be estimated as $x = \delta T/\Delta T \approx (2/\beta)\delta c/\Delta c$. Here δT is the undercooling below the coexistence temperature, δc is the excess concentration over the equilibrium concentration (Fig. 2), and $\beta = 0.325$. The LS theory gives the nucleation rate dN/dt (rate of formation of critical nucleus per unit volume) as a function of the supersaturation $x(t)$ in the scaled form

$$J(y) \approx dn/dt^* = AF(y)\exp(-1/y)^2. \quad (1)$$

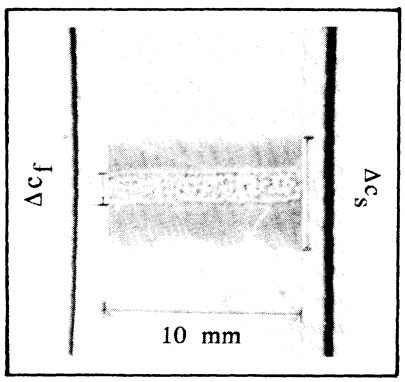

FIG. 1. A typical photograph of phase separation under a concentration gradient. The tilted lines are the grid shadows used to measure the gradient [10].

The variable $y = x/x_0$ is the scaled supersaturation ($x_0 = 1.24$ for binary liquids) and the reduced number density is $n = 64\pi\xi^3 N/x_0$. $t^* = t/\tau$ is the reduced time with the correlation time $\tau = 6\pi\eta\xi^3/k_B T$; η is the shear viscosity and k_B is the Boltzmann constant. The function $F(y)$ is weakly y dependent at small y and plays a minor role in the nucleation kinetics. A is a constant with a value close to 3.

Close to the critical point, the growth is affected due to the critical slowing down. Since in general experimentalists cannot separate nucleation from growth [1], LS introduce the half-completion time t_c^* at which supersaturation decreases to half of its initial value y_1,

$$t_c^* \approx (A'/y_1 J^2)^{0.2}. \quad (2)$$

The constant A' is of order 0.3 and J is evaluated from Eq. (1) with $y = y_1$. This universal behavior predicts a rather rapid completion of the phase separation at large y_1 values, where y_1 is expected to decrease almost linearly as $\ln t_c^*$.

In our experiment, the increasing width Δc_s of the slow zone corresponds to the "visibility" of newer nucleations for concentrations corresponding to lower y_1 values. Here $y_1 = (\Delta c - \Delta c_s)/\beta x_0 \Delta c$. For each y_1 we can measure a time at which droplets become visible. We tentatively identify this time as the half-completion time t_c^* and attempt to compare its behavior with that expected from LS theory. Note that the difference between the absolute values of the scaled time as defined by LS and by us is not very important considering the exponential behavior of the nucleation rate and the approximate pre-

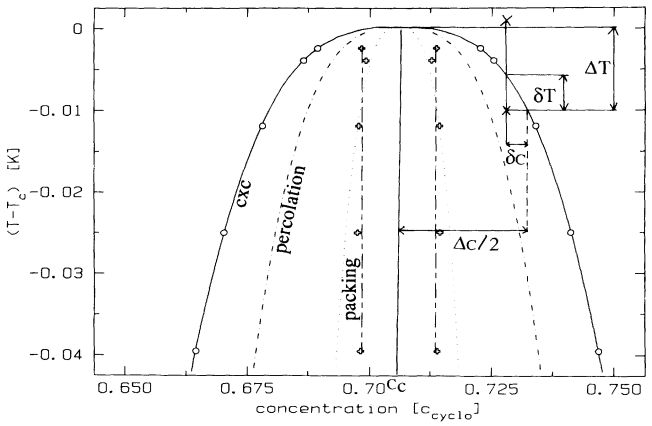

FIG. 2. Experimental miscibility gap of CC*M up to 40 mK below T_c. The solid curve is the known coexistence curve, which corresponds to the final value of the slow zone within 5% experimental uncertainty (open circles). Here we have normalized these final values to the coexistence curve. The plusses are the fast zone data and the dashed line is the extrapolated value of Δc_f ($=0.015$) at $t^* = 1$ (see Fig. 3). The various boundaries correspond to different theoretical limits expected for the ratio $\Delta c_f/\Delta c$ (dash-dotted curve: percolation limit, $\Delta c_f/\Delta c = 0.7$, and dotted curve: random packing limit, $\Delta c_f/\Delta c = 0.3$).

factors of the LS theory.

In Fig. 3 y_1 is plotted with respect to $\ln t_c^*$. It is clear that the data show the expected qualitative behavior with an almost linear region at small times and saturating to the equilibrium value zero at large times. These completion curves show a weak quench depth dependence at small times. Although it is not expected from scaling arguments, it seems to be consistent with the observations of the fast zone as we explain below.

The inset of Fig. 3 shows the fast zone width Δc_f over two decades of time for all the quenches. One sees that Δc_f is nearly independent of time and of the quench depth within the experimental uncertainty. A linear fit of Δc_f versus time shows a very small negative slope. Its extrapolation to $t^*=1$ gives $\Delta c_f=(1.5\pm0.3)\times10^{-2}$ as the average value for all the quenches (Fig. 2). Since binary liquids do not follow mean-field critical behavior within the present quench depths, it is inappropriate to compare the fast zone width with the classical spinodal line. In Fig. 2 the dash-dotted curve is the boundary of $\Delta c_f/\Delta c=0.70$ which is the three-dimensional continuum percolation limit of 15% by volume. A crossover at this threshold was expected [5] due to flow in percolating clusters. The fast zone is definitely much smaller than this percolation limit.

We believe that this finding is in accord with the recent picture of spinodal decomposition as a generalized nucleation process [3]. In predicting a smooth boundary between zones of spinodal decomposition and nucleation and growth, Binder argues that in the unstable region of the miscibility gap the activation energy ΔE^* for the formation of a critical nucleus R^* is $\Delta E^*\approx k_BT$ with $R^*\approx\xi$. In nucleation theories, ΔE^* is of order k_BT/y^2 and the critical radius R^* is of order $2\xi/y$. One then sees that the boundary between SD and nucleation and growth should correspond to $y\approx2$. In Fig. 3 we show the extrapolation of the linear fits to the completion curves. For the smaller quenches we find $y_1\approx2.4$ at $t_c^*=1$, close to the expected value of 2. This implies that the phase separation at $t_c^*=1$ corresponds to nucleation and growth with fluctuations of length ξ acting as critical nuclei and driving the phase separation process. This should be the fast zone limit. The accuracy of the present data is not enough to determine the precise quench depth dependence of y_1 at $t_c^*=1$. However, its increase with quench depth suggests the observed constancy of the fast zone, $\Delta c_s(t_c^*=1)=\Delta c_f=$const. For example, a variation of $y_1(t_c^*=1)$ from 1.7 to 2.5 as the quench depth increases from 2.4 to 40 mK gives $\Delta c_s(t_c^*=1)\approx0.015$, which is in fact the average fast zone width. This continuation of the slow zone nucleation and growth behavior into the fast zone strongly suggests that generalized nucleation is the phase separation process in the unstable region.

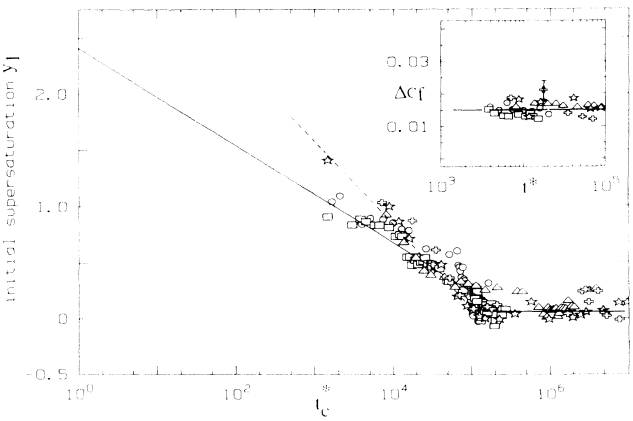

FIG. 3. Initial supersaturation y_1 plotted against $\ln t_c^*$ for all the quench depths (circles, 2.4 mK; squares, 4 mK; triangles, 12 mK; stars, 25 mK; plusses, 40 mK). The lines are fits to the linear region. Inset: Concentration width Δc_f at all the quench depths vs t^*. The dashed line is a fit linear in $\ln t^*$. The vertical bar is the estimated error.

Although our observations are qualitatively consistent with a constant Δc_f as discussed above, we cannot rule out completely a quench-depth-dependent fast zone corresponding to $y_1\approx2$, i.e., $\Delta c_f/\Delta c\approx0.3$, as shown in Fig. 2. This corresponds to a volume fraction of 0.35 which is close to the three-dimensional random packing limit (0.40). The enhanced coalescence of domains at the above volume fractions could be the origin of the striking contrast between the morphologies of the fast and slow zones (Fig. 1). As a matter of fact, the computer simulations by Rogers and Desai [13] also show this same change of morphology, when $\Delta c_f/\Delta c$ changes from 0.1 to 0.4.

When considering the kinetics of phase separation, Fig. 1 clearly indicates a gap in the growth rate for near-critical and off-critical concentrations. In our preliminary small-angle light scattering experiments, the laser beam of 0.3 mm width is scanned across the height of the sample from the instant it is quenched. The ring pattern is video recorded. In Fig. 4 the average radius K_m $(=2\pi/L_m)$ at the maximum intensity of the scattering ring is plotted in units of ξ $(K_m^*=K_m\xi)$ versus the reduced time t^* for $\Delta T=2.4$ mK along with the master curve. The growth exponent θ is $\theta=0.8+0.1$ for the fast zone, which corresponds to the effective exponent in this t^* range [4]. The slow zone gives $\theta=0.38\pm0.1$, whose extrapolation to $t^*=1$ gives $K_m^*\approx1$, as the fast growth master curve. Although these experiments are rather too preliminary for accurate quantitative details, the jump in the exponent value as concentration varies from critical to off critical is clearly in contrast with a continuous variation of θ from 1 to $\frac{1}{3}$. The inset in Fig. 4 shows the jump in the θ value for the concentration range studied.

Experiments with a concentration gradient therefore enable phase separation to be observed simultaneously at different volume fractions and supersaturations. Our findings are in agreement with generalized nucleation as the phase separation mechanism. The dependence of the

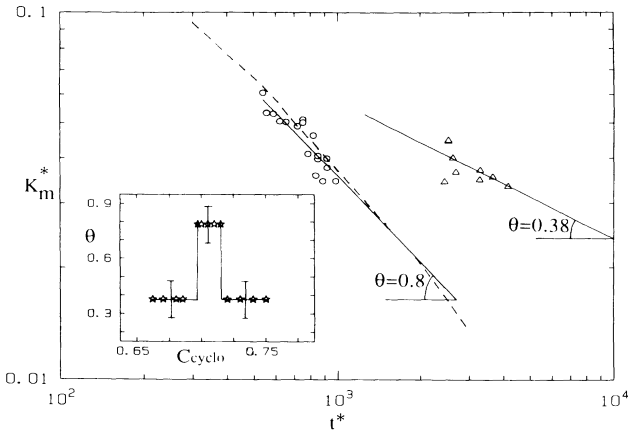

FIG. 4. Light scattering data: scaled wave vector K_m^* vs the reduced time t^* for $\Delta T = 2.4$ mK. Circles (triangles) refer to different heights in the fast (slow) zone. Solid lines are linear fits. Dashed line is the master curve for $c = c_c$ (from Ref. [4]). Inset: Schematic representation to show the jump in the growth exponent value θ for the range of concentrations scanned by the laser beam.

morphology and the growth exponent on volume fraction is abrupt and leads to a fast growth zone (exponent ≈ 1) and a slow growth zone (exponent $\approx \frac{1}{3}$). Our data indicate that the fast growth zone boundary is nearly temperature independent. However, we cannot completely exclude a weak temperature dependence corresponding to a boundary at 0.35 volume fraction. This is close to the 3D random packing limit where the droplet interconnection should accelerate the growth.

We thank J. F. Gouyet for the discussions at Djerba (Tunisia). We thank C. M. Knobler and our colleagues F. Perrot, R. Aschauer, T. Baumberger, and P. Guenoun for the discussions and useful suggestions. The financial support by CNES during this work is gratefully acknowledged. Service de Physique de l'Etat Condensé is a laboratoire de la Direction des Sciences de la Matière du Commissariat à l'Energie Atomique.

[a]Present address: Laboratoire de Physique Statistique, Ecole Normale Supérieure, 24 rue Lhomond, 75231, Paris CEDEX, France.

[b]Present address: Département de Physique Atomique et Moléculaire, Campus de Beaulieu, 35042 Rennes CEDEX, France.

[1] J. D. Gunton, M. San Miguel, and P. S. Sahni, in *Phase Transitions and Critical Phenomena*, edited by C. Domb and J. L. Lebowitz (Academic, New York, 1983), Vol. 8, pp. 277–465, and references therein.

[2] J. W. Cahn and J. E. Hilliard, J. Chem. Phys. **28**, 258 (1958); **31**, 688 (1959).

[3] K. Binder, Phys. Rev. A **29**, 341 (1984); in *Material Science and Technology: Phase Transitions in Materials*, edited by P. Haasen (VCH Verlagsgesellschaft Weinheim, Germany, 1991), Vol. 5. pp. 405–471, and references therein.

[4] D. Beysens, F. Perrot, and P. Guenoun, Phys. Rev. A **32**, 1818 (1985).

[5] E. D. Siggia, Phys. Rev. A **20**, 595 (1979).

[6] N. C. Wong and C. M. Knobler, Phys. Rev. A **24**, 3205 (1981).

[7] M. Kolb, T. Gobron, J. F. Gouyet, and B. Sapoval, Europhys. Lett. **11**, 601 (1990).

[8] A. G. Aizpiri, R. G. Rubio, and M. D. Pend, J. Chem. Phys. **88**, 1934 (1988).

[9] N. C. Wong and C. M. Knobler, J. Chem. Phys. **69**, 725 (1978).

[10] V. Gurfein and D. Beysens, Opt. Commun. **85**, 147 (1991).

[11] Y. Jayalakshmi and D. Beysens (to be published).

[12] J. S. Langer and A. J. Schwartz, Phys. Rev. A **21**, 948 (1980).

[13] T. M. Rogers and Rashmi C. Desai, Phys. Rev. B **39**, 11956 (1989).

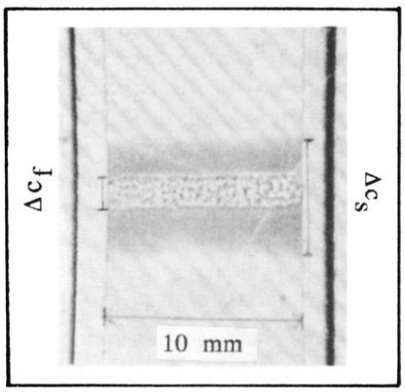

FIG. 1. A typical photograph of phase separation under a concentration gradient. The tilted lines are the grid shadows used to measure the gradient [10].